The Astronomical Journal, 125:2721–2727, 2003 May

ESO LARGE PROGRAMME ON TRANS-NEPTUNIAN OBJECTS AND CENTAURS: SPECTROSCOPIC INVESTIGATION OF CENTAUR 2001 BL_{41} AND TNOs (26181) 1996 GQ_{21} AND (26375) 1999 DE_9[1]

A. Doressoundiram,[2] G. P. Tozzi,[3] M. A. Barucci,[2] H. Boehnhardt,[4] S. Fornasier,[5] and J. Romon[2]

Received 2003 January 3; accepted 2003 February 5

ABSTRACT

Observational results that are part of an ESO Large Programme dedicated to the characterization of the physical properties of trans-Neptunian objects and Centaurs are presented. We report observations related to the Centaur 2001 BL_{41} and two trans-Neptunian objects, (26181) 1996 GQ_{21} and (26375) 1999 DE_9. We present results from broadband photometry (*JHK* filters) and low-dispersion infrared spectroscopy performed with ISAAC at the Very Large Telescope, in Chile. None of the spectra show evidence of absorption features—in particular, water ice features. We use a radiative transfer model to investigate the surface composition of these icy and primitive outer solar system bodies. We suggest models composed of geographical mixtures of organic compounds and minerals.

Key words: Kuiper belt — minor planets, asteroids — techniques: photometric — techniques: spectroscopic

1. INTRODUCTION

The trans-Neptunian objects (TNOs), also called Edgeworth-Kuiper objects, orbit beyond Neptune and consist of icy bodies that are considered among the most pristine solar system objects observable from Earth. Particular dynamical classes of these objects are the Centaurs and the scattered-disk objects, which both have very eccentric orbits. They may play an important role in understanding the transfer rate and evolution of objects between orbital classes in the outer solar system. To date (2003 February), 125 objects belong to this peculiar class, and they form a group apart in the lists of the Minor Planet Center.[6]

The Centaurs are a dynamical class of bodies on unstable orbits (Holman & Wisdom 1993) whose semimajor axes fall between those of Jupiter and Neptune. Their dynamical lifetimes are measured in millions of years. Long-term orbital integration of TNOs suggests that perturbations by the giant planets or mutual collisions could provide a source of Centaurs and short-period comets (Duncan, Levison, & Budd 1995; Levison & Duncan 1997). According to Levison, Dones, & Duncan (2001), some of the Centaurs may have instead originated in the Oort cloud. The first object discovered in this group was Chiron, when it was near the orbit of Uranus at 18 AU (Kowal 1978), and at present it is the only object (along with comet P/Schwassmann-Wachmann 1) of this population showing the existence of temporally variable cometary activity.

The scattered objects have large, highly eccentric, and highly inclined orbits. This class was established in 1996 October with the discovery of the first object, 1996 TL_{66} (Luu et al. 1997). The most distant such object discovered to date (2000 OO_{67}) has an aphelion at 1034 AU. The external boundaries of this population are not yet known, because of the difficulty in detecting these distant objects, but they probably extend to the Oort cloud. These objects are thought to represent the population of scattered planetesimals from the early stages of the solar system (Torbett 1989; Ip & Fernández 1991; Duncan & Levison 1997), in a scenario where Uranus and Neptune scattered many planetesimals to large distances.

There is strong interest in studying the physical properties and nature of this population, which can provide information about the primordial processes that dominated the early solar nebula. Unfortunately, very few data are presently available on the physical properties of these bodies (see Barucci, Doressoundiram, & Cruikshank 2003 for a complete review), mostly because of their faintness. Dedicated visible and infrared observations of these objects were part of a Large Programme carried out at ESO Chile (Boehnhardt et al. 2002; Barucci et al. 2002) to improve our knowledge of the nature of TNOs.

The observational results presented in this paper are part of this ESO Large Programme. In this work, we present the observational results (visible and infrared spectroscopy and photometry), as well as tentative models of the surface composition of the observed objects.

2. OBSERVATIONS AND DATA REDUCTION

We observed the Centaur 2001 BL_{41} and two TNOs, (26181) 1996 GQ_{21} and (26375) 1999 DE_9. In this paper, we present results from broadband photometry (*JHK* filters) and low-dispersion infrared spectroscopy performed at the ESO's Very Large Telescope (VLT), in Chile. Observations, aspect data, and weather conditions are reported in Table 1.

2.1. *Near-Infrared Photometry*

The near-infrared photometric measurements reported here were recorded with the ISAAC instrument on the 8 m Unit Telescope 1 of the VLT on 2002 February 18–21. We

[1] Based on observations collected at the European Southern Observatory, Paranal, Chile (program 167.C-0340).

[2] Laboratoire d'Etudes Spatiales et d'Instumentation en Astrophysique, Observatoire de Paris, F-92195 Meudon Principal Cedex, France; Alain.Doressoundiram@obspm.fr.

[3] Osservatorio Astrofisico di Arcetri, INAF, Largo Enrico Fermi 5, I-50125 Firenze, Italy.

[4] Max-Planck-Institut für Astronomie, Königstuhl 17, D-69117 Heidelberg, Germany.

[5] Dipartimento di Astronomia, Università di Padova, vicolo dell'Osservatorio 2, I-35122 Padova, Italy.

[6] See http://cfa-www.harvard.edu/iau/lists/Centaurs.html.

TABLE 1
ASPECT DATA AND WEATHER CONDITIONS DURING OBSERVATIONS

Object	Dynamical Class	Date (UT)	r (AU)	Δ (AU)	α (deg)	Observations	Weather
(26181) 1996 GQ_{21}	Scattered	2002 Feb 18	39.43	39.01	1.31	*H* spectroscopy	Thin cirrus
		2002 Feb 19	39.43	38.99	1.30	*JK* photometry	Thin cirrus
						H spectroscopy	
		2002 Feb 21	39.43	38.96	1.28	*JK* photometry	Clear
						JK spectroscopy	
(26375) 1995 DE_9	Scattered	2002 Feb 20	34.18	33.20	0.22	*JHK* photometry	Photometric
						H spectroscopy	
2001 BL_{41}	Centaur	2002 Feb 18	8.45	7.51	2.30	*JH* spectroscopy	Thin cirrus
		2002 Feb 19	8.45	7.52	2.42	*JHK* photometry	Thin cirrus
						HK spectroscopy	
		2002 Feb 21	8.45	7.54	2.64	*JHK* photometry	Clear
						K spectroscopy	

NOTE.—The quantities r, Δ, and a are respectively the heliocentric distance, topocentric distance, and phase angle of the object, from the Minor Planet Center's ephemeris service.

recorded series of images in the J, H, and K_s filters, centered at 1.25, 1.65, and 2.16 μm, respectively, before each spectroscopic observation. For each target, a set of images moved in a dither pattern was recorded, as is common in infrared photometric acquisition.

Only one night was photometric (February 20), and we observed several infrared photometric standard stars (Persson et al. 1998) for photometric calibration. The night of February 19 was not photometric, so we performed photometric measurements relative to some field stars that were observed again the following nights. The night of February 21 was clear but with high humidity, and the photometric calibration was performed using the zero points and extinction coefficients provided by ESO on the basis of standard reduction procedures applied to two standard stars observed during the night.

The photometric reduction was performed using the "jitter" routine of the Eclipse package and the ESO MIDAS software, following the data processing steps described in Romon et al. (2001) for image combination and sky subtraction. The magnitudes of stars and objects were finally measured using classical aperture photometry for each filter. The results of our photometric measurements are listed in Table 2.

The object 1999 DE_9 was observed in photometric conditions. Measurements in J, H, and K_s were obtained once, during the night of February 20. Centaur 2001 BL_{41} was observed two times, on both the night of February 19 and that of February 21. The magnitudes from the first night (not photometric) were computed via relative photometry with respect to three field stars observed and calibrated during the photometric night of February 20. Magnitudes from the second night were derived directly and calibrated using the zero points and extinction coefficients provided by ESO.[7] Magnitudes for 1996 GQ_{21} were computed only in the J and K_s filters, both by direct photometry the night of February 21 and by relative photometry the night of February 19. (The three field stars used were observed again and calibrated the night of February 21.)

[7] See http://www.eso.org/observing/dfo/quality/ISAAC/img/trend/p68/trend_SIZP_current.asc.

TABLE 2
PHOTOMETRIC OBSERVATIONS AND RESULTS

Object	Date	Filter	UT Start	T_{exp} (s)	Magnitude	Colors
(26181) 1996 GQ_{21}	2002 Feb 19	*J*	0658	90	19.18 ± 0.07	
		K_s	0725	100	18.39 ± 0.09	$J-K = 0.79 \pm 0.11$
	2002 Feb 21	*J*	0857	90	19.23 ± 0.04	
		K_s	0903	100	18.47 ± 0.06	$J-K = 0.76 \pm 0.07$
(26375) 1999 DE_9	2002 Feb 20	*J*	0251	90	18.80 ± 0.04	
			0340	90	18.83 ± 0.04	
		H	0255	50	18.51 ± 0.05	$J-H = 0.29 \pm 0.06$
		K_s	0310	100	18.46 ± 0.05	$J-K = 0.36 \pm 0.06$
2001 BL_{41}	2002 Feb 19	*J*	0115	90	19.16 ± 0.05	
			0605	90	19.15 ± 0.05	
		H	0120	50	18.80 ± 0.05	$J-H = 0.36 \pm 0.07$
		K_s	0135	100	18.48 ± 0.09	$J-K = 0.68 \pm 0.10$
	2002 Feb 21	*J*	0220	90	19.14 ± 0.05	
		H	0204	50	18.77 ± 0.05	$J-H = 0.37 \pm 0.07$
		K_s	0143	100	18.56 ± 0.05	$J-K = 0.58 \pm 0.07$

TABLE 3
SPECTROSCOPIC OBSERVATIONS

OBJECT	DATE	UT START	AIR MASS Start	AIR MASS End	SPECTRAL BAND	T_{exp} (minutes)
(26181) 1996 GQ_{21}	2002 Feb 18	0701	1.18	1.04	*H*	120
	2002 Feb 19	0743	1.08	1.04	*H*	78
	2002 Feb 21	0555	1.39	1.15	*J*	60
		0717	1.12	1.04	*K*	30
(26375) 1999 DE_9	2002 Feb 20	0352	1.25	1.20	*H*	120
2001 BL_{41}	2002 Feb 18	0158	1.20	1.23	*J*	42
		0319	1.23	1.48	*H*	108
	2002 Feb 19	0245	1.24	1.23	*H*	60
		0403	1.24	1.58	*K*	90
	2002 Feb 21	0420	1.29	1.49	*K*	54

2.2. *Near-Infrared Spectroscopy*

Near-infrared spectroscopic measurements were performed using ISAAC in its low-resolution spectroscopic mode. We used a slit width of 1″, oriented at the parallactic angle, when we were observing at an air mass greater than 1.5. Each *J*, *H*, and *K* spectrum was obtained separately. The resulting spectral resolution was about 500. The observations were done by nodding the object along the slit in two different positions (A and B) separated by ~10″. Solar-analog stars observed at similar air masses as the objects were obtained in order to remove the solar contribution. Several solar analogs were compared and found to give very similar results. Thus, we used an average of the solar analogs Landolt 98-978, HD 28099, and HD 147284 to compute the reflectivity spectrum of each object, except for the night of February 20, for which we used only one solar analog (HD 147284). We could not obtain *J* and *K* spectra for 1999 DE_9, because of technical problems with ISAAC, during the night of February 20.

The spectroscopic data were reduced using the Eclipse package and the MIDAS software. The basis of the data reduction process is to combine pairs of image differences (e.g., A − B and B − A) in order to properly remove the sky contribution and obtain an improved signal-to-noise ratio (S/N). For details of the method, see Romon et al. (2001). Because of the imperfect and variable weather conditions, all the resulting single spectra were checked, and those with very low S/N were discarded from the image combination process. Table 3 gives the details of the spectroscopic observations along with the effective exposure time. As a result of object visibility, combined with some technical problems with ISAAC, we could not obtain all of the *J*, *H*, and *K* spectra for each object on a single night. In addition, the *H* and *K* of spectra of 2001 BL_{41} were obtained on two nights, as was the *H* spectrum of 1996 GQ_{21}.

2.3. *Visible Photometric Data*

Visible spectra of the same three objects were obtained during the same observing campaign and have been published in a previous paper (Lazzarin et al. 2003). However, the accompanying visible photometric observations could not be performed during our observing run, because of the nonphotometric conditions. This is a real handicap, since we need at least the *V*−*J* colors to connect the visible and infrared spectra and properly reproduce the spectral slope, which can be quite steep for outer solar system objects. To partly alleviate this problem, we used the available data published so far, as discussed in the next section.

3. RESULTS

The *JHK* photometry that we obtained is reported in Table 2. A broadband *V* measurement was unavailable for our observations. So, to compute the *V*−*J* color, one solution would be to use published data for the reduced *V* magnitude of a given object. However, by doing so we encounter two important problems that may have devastating errors in the resulting *V*−*J* color. The first is the brightness variation caused by a nonspherical rotating body, and the second is the opposition-brightening effect.

Regarding the first problem, it has become more and more obvious with recent work on light-curve studies of TNOs that nonsimultaneous data suffer the ever-present risk of being distorted either by color variations with rotation or by light-curve effects (see, e.g., the TNO light-curve investigation of Sheppard & Jewitt 2002). The second problem, the opposition-brightening effect, may also be significantly important, especially for low-albedo objects with porous surfaces. This effect has been widely studied in asteroids (Belskaya & Shevchenko 2000). Recently, Sheppard & Jewitt (2002) analyzed the phase curves of seven TNOs in the phase-angle range $0^\circ \leq \alpha \leq 2^\circ$. They found rather steep slopes for their whole TNO sample, compatible with a moderate opposition surge. This discovery shows that we may introduce a systematic error when computing visible-infrared color by combining measurements from different epochs.

That is why we took for the *V*−*J* colors of 1999 DE_9 and 1996 GQ_{21} the measurements of McBride et al. (2003). These have the significant benefit of having been taken at both visible and infrared wavelengths simultaneously and are thus potentially free of any systematic errors introduced by either phase-angle or rotational effects. To compute the *V*−*H* and *V*−*K* colors, we used both our *J*−*H* and *J*−*K* colors and the *V*−*J* color of McBride et al. By doing so, we are implicitly assuming that the TNOs' surfaces are compositionally homogeneous, which is not obvious at all. Table 4 summarizes the color information for each object.

The reduced infrared spectra of the three objects, (26181) 1996 GQ_{21}, (26375) 1999 DE_9, and 2001 BL_{41}, are presented in Figure 1. We combined the individual *H* and *K* spectra of 2001 BL_{41} obtained on two nights, as well as the *H* spectrum

TABLE 4
MEAN COLORS

Object	$V-J$	$J-H$[a]	$J-K$[a]
Solar colors	1.08	0.29	0.35
(26181) 1996 GQ_{21}	2.44 ± 0.06[b]	...	0.77 ± 0.06
(26375) 1999 DE_9	1.89 ± 0.07[b]	0.29 ± 0.06	0.36 ± 0.06
2001 BL_{41}	1.65 ± 0.07[c]	0.37 ± 0.05	0.61 ± 0.06

[a] When multiple colors were available, a weighted mean was computed. Solar colors are from Hardorp 1980 and Hartmann et al. 1982.
[b] Simultaneous $V-J$ color measurement from McBride et al. 2003.
[c] $V-J$ color computed with the photometric measurements of Bauer et al. 2003.

of 1996 GQ_{21}, because individual spectra had too low S/N to be useful alone. The spectra of the objects have been divided by the spectrum of the Sun and normalized to unity at around the central wavelength of the corresponding spectral band. The original spectra were smoothed by Gaussian filtering, resulting in a final spectral resolution of 200. As a result of the specific operational mode of ISAAC, the different J, H, and K spectra were obtained separately, so that the three spectra have to be adjusted with the accompanying photometric measurements in the J, H, and K_s filters.

None of the spectra show evidence of any spectral features, given the S/N obtained so far. In particular, there are no absorption bands at 1.5 and 2.0 μm, the diagnostic bands of water ice, which is currently the most commonly detected material on outer solar system bodies.

In Figures 2, 3, and 4, the infrared spectra are shown along with the visible spectrum from Lazzarin et al. (2003). In order to obtain useful spectral information, we improved the S/N by smoothing the original ISAAC spectra with a Gaussian filtering of $\sigma = 15$ pixels. The resulting infrared spectra have a final spectral resolution of 100 in J, H, and K. The edges of each spectral region have been cut to avoid low-S/N spectral regions. The different spectral ranges have been adjusted using the photometric observations in V, J, H, and K (see Table 4), transformed in reflectivity using solar values (Hardorp 1980; Hartmann, Cruikshank, & Degewij 1982).

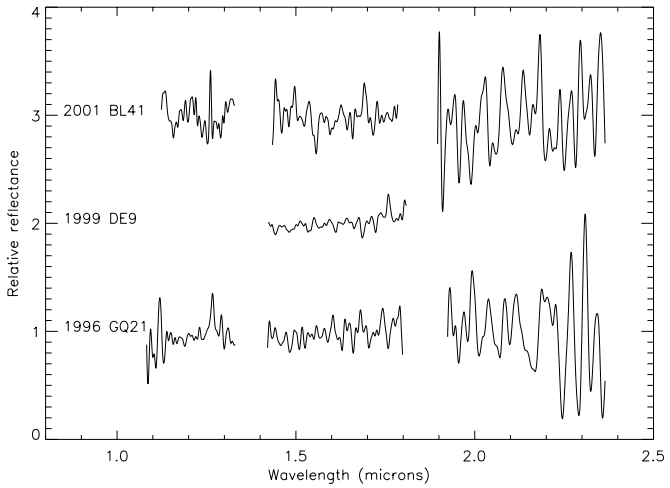

FIG. 1.—Relative reflectance spectra of 1996 GQ_{21}, 1999 DE_9, and 2001 BL_{41}. The J spectra are normalized around 1.25 μm, the H around 1.65 μm, and the K around 2.16 μm. The spectrum of each object has been shifted by 1 unit for clarity.

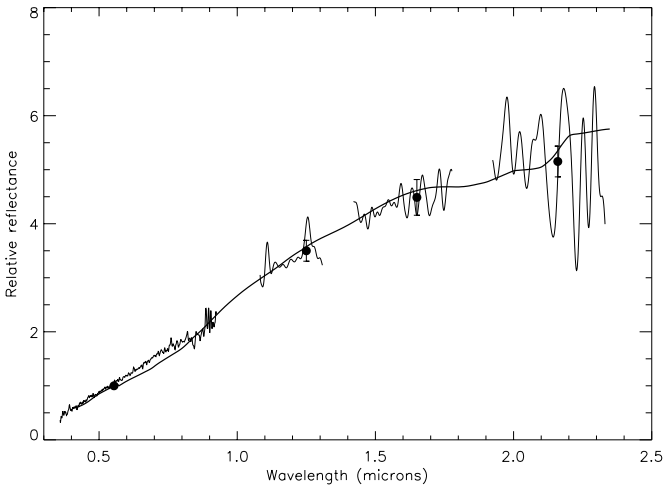

FIG. 2.—Spectra of 1996 GQ_{21} in the V, J, H, and K ranges. The spectra have been adjusted using the photometric V, J, H, and K_s colors and have been normalized to 1 at 0.55 μm. The compositional model shown (*heavy solid line*) is composed of 15% Titan tholin, 35% ice tholin, and 50% amorphous carbon. The mean optical albedo at V-band wavelengths is 0.05. The visible spectrum is from Lazzarin et al. (2003), and the $V-J$ color is from McBride et al. (2003).

In order to reproduce the spectral behavior of these objects, we used a radiative transfer model (Douté & Schmitt 1998). This model is similar to the Hapke model and, in particular, is subject to the same limitation that the particle sizes must be significantly greater than the wavelength of the scattered light. The goal of modeling the spectral reflectance is to derive information on these objects' composition and surface microstructure. We propose synthetic spectra of several geographical (spatial) mixtures of complex organic compounds (tholins, kerogen), dark material (amorphous carbon), and silicates (tremolite). However, we would like to stress that the models proposed in Figures

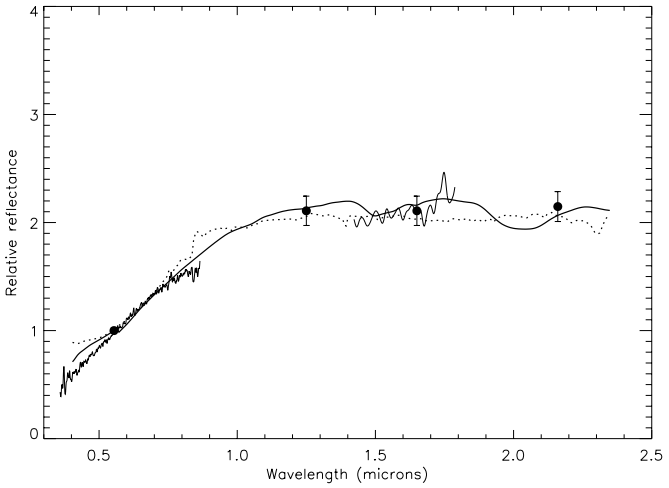

FIG. 3.—Same as Fig. 2, but for 1999 DE_9 in the V and H ranges. Two compositional models are proposed. One (*heavy solid line*) is composed of 24% Titan tholin, 15% ice tholin, 54% amorphous carbon, and 7% water ice. The mean optical albedo at V-band wavelengths is 0.10. The second suggested model (*dotted line*) is composed of 99% kerogen and 1% tremolite. The mean optical albedo at V-band wavelengths is 0.02.

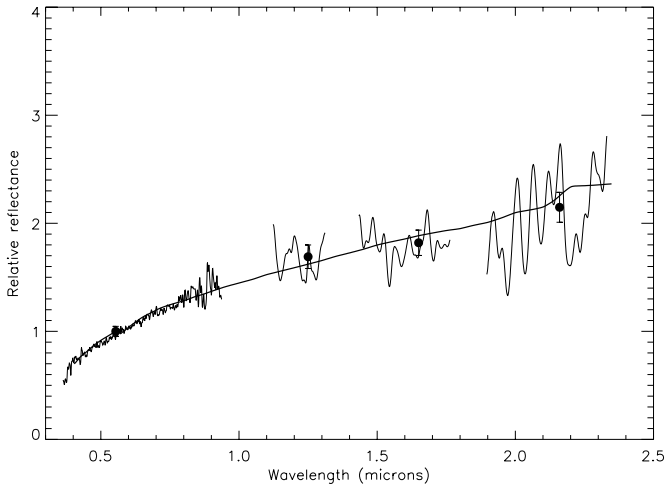

FIG. 4.—Same as Fig. 2, but for 2001 BL_{41}. The compositional model (*heavy solid line*) is composed of 17% Triton tholin, 10% ice tholin, and 73% amorphous carbon. The mean optical albedo at *V*-band wavelengths is 0.08.

2–4 are only suggestions of what might be the nature of the surface material present in small outer solar system bodies. These solutions are not unique, given the many unknown parameters needed to constrain the models. However, we have potentially at our disposal several parameters to constrain our modeling. These are the geometric albedo, the spectral gradient, and the presence or absence of absorption bands arising from minerals, ices, and organic solids. First, in the present work, the lack of albedo information for our objects eliminates one important constraint on the modeling, but under the assumption of a low albedo, surface models have been computed to interpret the general behavior of the spectrum. Secondly, given the absence of absorption features in our infrared spectra (which, however, constitutes a constraint), the spectral gradient is indeed our prime constraint, especially the visible-infrared gradient. The superposed dotted and heavy solid lines in Figures 2–4 represent the computed models.

4. DISCUSSION

4.1. (*26181*) *1996 GQ_{21}*

The object (26181) 1996 GQ_{21} is a scattered-disk TNO. We present here the first infrared spectra (Fig. 1) in the *J*, *H*, and *K* bands. The visible spectrum has been obtained by Lazzarin et al. (2003) in the course of the same ESO Large Programme. With a visible spectral gradient of 34.9% per 100 nm, 1996 GQ_{21} is a significantly red object. The photometric measurements obtained in the *J* and K_s broadband filters indicate that the red gradient extends to infrared wavelengths. The *H* magnitude could not be obtained, as a result of technical problems. It is noteworthy that the two *J* measurements, as well as the two *K* measurements, obtained at different epochs do not show any significant variations (Table 2). Sheppard & Jewitt (2002) investigated the rotational light curve of this object in the visible range. They found no measurable photometric variations over a period extending 24 hr. This is consistent with, though not proving, the possibility that the light curve may be flat as well in the *J* and *K* bands.

Figure 2 shows our ISAAC spectra along with the visible spectrum of Lazzarin et al. (2003). The spectra have been adjusted using the *V*−*J* color of McBride et al. (2003) and our *J* and *K* measurements. The heavy solid line in Figure 2 is our proposed best solution for the surface composition of 1996 GQ_{21}. The model is a geographical mixture composed of 15% Titan tholin, 35% ice tholin, and 50% amorphous carbon. The grain size is 10 μm for the three components. The mean optical albedo at *V*-band wavelengths is 0.05. To obtain this model, we tried several combinations of minerals, organics, and ices. We introduced tholin material into our model to fit the red spectral gradient that usually characterizes outer solar system bodies' spectra. Tholins are synthetic macromolecular compounds produced from irradiated gaseous or solid mixtures of simple hydrocarbons, water, or nitrogen (Sagan & Khare 1979). Though their optical properties depend on the original mixture and conditions of irradiation, all tholins show common characteristics: a red spectral gradient and a low albedo. In the suggested model for the composition of 1996 GQ_{21}, we introduced Titan tholin (Khare et al. 1984) to reproduce the redward gradient that extends beyond 0.6 μm and ice tholin I (Khare et al. 1993) to fit the red slope shortward of 0.6 μm, which was not reproduceable with the Titan tholin. Finally, the addition of amorphous carbon improved the general fit of the spectra.

4.2. (*26375*) *1999 DE_9*

The TNO (26375) 1999 DE_9 is a scattered-disk object. The spectral gradient (25.5% per 100 nm) at visible wavelengths indicates a red object (Lazzarin et al. 2003). The ISAAC infrared colors, *J*−*H* and *J*−*K* (see Table 4), indicate that the red color gradient does not extend to infrared wavelengths and that the reflectance of 1999 DE_9 is quite flat longward of *J* wavelengths.

The infrared spectrum of 1999 DE_9 has been obtained previously at the Keck Telescope by Jewitt & Luu (2001) in the 1–2.5 μm range. Their spectrum showed solid-state absorption features near 1.4, 1.6, 2.00, and probably 2.25 μm. The location of these bands has been tentatively interpreted by Jewitt & Luu as evidence of the hydroxyl group, with possible interaction with an Al or Mg compound. The strongest water band at 2.00 μm is only about 10% deep. The presence of the drop from 1.3 to 1 μm seems to be consistent with olivine absorption. If the presence of the hydroxyl group is confirmed, this may imply the presence of liquid water and a temperature near the melting point for at least a short period of time. However, the visible spectrum of Lazzarin et al. does not show any evidence of aqueous altered materials (0.7 μm absorption feature). In the limited spectral range of our *H*-band spectrum, we could not confirm the detection of the 1.6 μm feature. However, our spectrum has a lower S/N than the Keck spectrum, and the 1.6 μm feature appeared very weakly in the Keck spectrum. Thus, the presence of this feature in our VLT spectrum cannot be ruled out. Interestingly, the slight spectral gradient in our 1.4–1.8 μm wavelength range is compatible with that of Jewitt & Luu. This makes plausible the presence of the 2 μm water band detected by those authors.

Figure 3 shows our ISAAC *H* spectrum along with the visible spectrum of Lazzarin et al. (2003). The spectra have been adjusted using the *V*−*J* color of McBride et al. (2003) and our *JHK* photometry. In a first attempt to model the spectral

behavior of 1999 DE_9, we consider only the limited spectral data we have. Indeed, with solely the *H*-band spectrum we do not have any indication of the presence or absence of water ice. Consequently, we propose a model (*dotted line*) composed of 99% kerogen (10 μm grain size) and 1% tremolite (large grain size). The mean optical albedo at *V*-band wavelengths is 0.02. Kerogens are complex organic compounds and have already been used to reproduce the red spectra of dark asteroids and Centaurs (Barucci et al. 2000). Terrestrial kerogens are the product of the decay (at high temperature and pressure) of organic matter, but interstellar dust and some carbonaceous meteorites contain materials of similar structure of nonbiological origin. In order to lower the reflectance around 1 μm and fit the value of the *J* reflectivity, we include some ferrous silicate in the model. This kind of mineral was suggested by Jewitt & Luu (2001) to explain the broad absorption in the 1–1.3 μm range present in the Keck spectrum. Forsterite (a magnesium-rich olivine) has previously been proposed to fit a 1 μm absorption in the spectrum of Centaur (5145) Pholus (Cruikshank et al. 1998). We tried several olivines to fit the spectral behavior around 1 μm, but our attempts failed in fitting the reflectance spectrum. We found a better match with another ferrous silicate, tremolite,[8] which is a calcium-magnesium silicate that is moderately hydrated. The reflectance spectrum of this mineral has a fairly prominent broad band near 1 μm, indicating that it contains some ferrous ion. It displays a very sharp band at 1.4 μm and less sharp bands between 2.0 and 2.5 μm, due to the overtone and combination tones of the OH stretch, respectively. In particular, the bands at 2.2 and 2.3 μm are due to combinations of the OH stretching modes with lattice modes. Given the very limited spectral range we have, especially in the infrared, this model composed of kerogen and tremolite seems to be a good compromise in fitting the reflectance spectrum of 1999 DE_9. However, these materials do not properly reproduce the spectral behavior shortward to 0.5 μm and around 0.8 μm.

Taking into consideration the fact that Jewitt & Luu (2001) found water ice in the spectrum of 1999 DE_9, we tried another model including some water ice. This model is a geographical mixture composed of 24% Titan tholin, 15% ice tholin, 54% amorphous carbon, and 7% water ice (Fig. 3, *heavy solid line*). The grain size is 10 μm for all components. The mean optical albedo at *V*-band wavelengths is 0.10. Tholins were required in order to reproduce the spectral slope, especially in the visible range. The small percentage of water ice appears satisfactory in reproducing the overall spectral behavior in the infrared range. In particular, it succeeds in reproducing the slight spectral gradient in the *H* band. The two proposed models are only suggestions, as too few spectral constraints are available for 1999 DE_9. Obviously, further observations are needed for this interesting object.

4.3. *2001 BL_{41}*

The object 2001 BL_{41}, classified as a Centaur, is moderately red according to the visible spectroscopic result of Lazzarin et al. (2003). Our photometric results confirm that this moderately red color gradient extends to infrared wavelengths (i.e., $J-H$ and $J-K$ colors). This object is the least studied of our selection. No $V-J$ color is known, or any rotational period. A very recent work by Bauer et al. (2003) reported no significant variation of the optical light curve over a time span of 2 hr. We have a concordant result from our infrared photometry; the *J* magnitude was almost constant on UT February 19 in two measurements 5 hr apart, and on February 21 (see Table 2). The same also applies for the *H* and *K* photometry. Bauer et al. also reported magnitudes and colors ($V-R = 0.52 \pm 0.06$) for 2001 BL_{41}. From their *R*-band phase curve, they derived Lumme-Bowell values of $G = 0.17 \pm 0.06$ and $H = 10.99 \pm 0.03$. We used these values to derive our own *V* magnitude at the date of our *J* photometry. We found $V = 20.80 \pm 0.05$ and computed a value for the $V-J$ color of 1.65 ± 0.05. This $V-J$ value should potentially be free of any systematic errors introduced by phase effects.

The whole spectrum of the object is presented in Figure 4, including the infrared spectra and the visible spectrum of Lazzarin et al. (2003). As was done for the previous objects, the spectra were adjusted by using the obtained infrared and visible photometry. To investigate the possible composition of 2001 BL_{41}, we ran the radiative transfer model. We found a geographical mixture composed of 17% Triton tholin, 10% ice tholin, and 73% amorphous carbon (*heavy solid line*), with a mean optical albedo at *V*-band wavelengths of 0.08. The grain size is 10 μm for the three components. The use of Triton tholin (McDonald et al. 1994) was adequate to reproduce the continuous and moderate gradient of the whole spectrum from 0.4 to 2.4 μm. Ice tholin I (Khare et al. 1993), as in the previous models, was useful to reproduce the gradient shortward of 0.6 μm, and finally, amorphous carbon helped to improve the general fit of the spectra.

5. CONCLUSIONS

We have obtained photometric and spectroscopic observations of one Centaur and two TNOs, observed at the VLT. We thus presented in this paper first results for the spectral reflectance of the Centaur 2001 BL_{41} and the scattered-disk objects (26181) 1996 GQ_{21} and (26375) 1999 DE_9 in the 0.4–2.4 μm wavelength range. All the spectra appear featureless. In particular, we did not find any evidence of water ice absorption features, with the exception of 1999 DE_9, for which our limited wavelength range does not allow definitive conclusions. Water ice is presumed to be the principal component of the bulk composition of outer solar system objects (formed mostly at the same low temperature of 30–40 K) and should constitute a large fraction of the bulk composition of this population. Water ice must be present on these bodies, even if it is not detectable in the spectra. The reasons why we systematically fail to detect water ice are not clear. The explanations generally invoked are the presence of coma, as in the case of 2060 Chiron (Luu, Jewitt, & Trujillo 2000), and the action of various processes of space weathering (due to solar radiation, cosmic rays, and interplanetary dust), which affect the uppermost layer of the surface (Strazzulla 1998).

Radiative transfer models to investigate the possible surface composition have been performed on the reflectance spectra. We suggest models composed of geographical mixtures of organic compounds (kerogen, tholins, amorphous carbon) and minerals (tremolite). Because of the lack of constraints, the obtained models give only an indication of the possible material present on the surface.

[8] US Geological Survey Digital Spectral Library: http://speclab.cr.usgs.gov/spectral-lib.html.

REFERENCES

Barucci, M. A., et al. 2002, A&A, 392, 335
Barucci, M. A., de Bergh, C., Cuby, J.-G., Le Bras, A., Schmitt, B., & Romon, J. 2000, A&A, 357, L53
Barucci, M. A., Doressoundiram, A., & Cruikshank, D. P. 2003, in Comets II, ed. M. Festou (Tucson: Univ. Arizona Press), in press
Bauer, J. M., Meech, K. J., Fernández, Y. R., Pittichova, J., Delsanti, A. C., Boehnhardt, H., & Hainaut, O. R. 2003, in preparation
Belskaya, I. N., & Shevchenko, V. G. 2000, Icarus, 147, 94
Boehnhardt, H., et al. 2002, A&A, 395, 297
Cruikshank, D. P., et al. 1998, Icarus, 135, 389
Douté, S., & Schmitt, B. 1998, J. Geophys. Res., 103, 31367
Duncan, M. J., & Levison, H. F. 1997, Science, 276, 1670
Duncan, M., Levison, H. F., & Budd, S. M. 1995, AJ, 110, 3073
Hardorp, J. 1980, A&A, 91, 221
Hartmann, W. K., Cruikshank, D. P., & Degewij, J. 1982, Icarus, 52, 377
Holman, M. J., & Wisdom, J. 1993, AJ, 105, 1987
Ip, W.-H., & Fernández, J. A. 1991, Icarus, 92, 185
Jewitt, D. C., & Luu, J. X. 2001, AJ, 122, 2099
Khare, B. N., Sagan, C., Arakawa, E. T., Suits, F., Callcott, T. A., & Williams, M. W. 1984, Icarus, 60, 127
Khare, B. N., Thompson, W. R., Cheng, L., Chyba, C., Sagan, C., Arakawa, E. T., Meisse, C., & Tuminello, P. S. 1993, Icarus, 103, 290
Kowal, C. T. 1978, The Sciences, 18, 12
Lazzarin, M., Barucci, M. A., Boehnhardt, H., Tozzi, G. P., de Bergh, C., & Dotto, E. 2003, AJ, 125, 1554
Levison, H. F., Dones, L., & Duncan, M. J. 2001, AJ, 121, 2253
Levison, H. F., & Duncan, M. J. 1997, Icarus, 127, 13
Luu, J., Marsden, B. G., Jewitt, D., Trujillo, C. A., Hergenrother, C. W., Chen, J., & Offutt, W. B. 1997, Nature, 387, 573
Luu, J. X., Jewitt, D. C., & Trujillo, C. 2000, ApJ, 531, L151
McBride, N., Green, S. F., Davies, J. K., Tholen, D. J., Sheppard, S. S., Whiteley, R. J., & Hillier, J. K. 2003, Icarus, 161, 501
McDonald, G. D., Thompson, W. R., Heinrich, M., Khare, B. N., & Sagan, C. 1994, Icarus, 108, 137
Persson, S. E., Murphy, D. C., Krzeminski, W., Roth, M., & Rieke, M. J. 1998, AJ, 116, 2475
Romon, J., de Bergh, C., Barucci, M. A., Doressoundiram, A., Cuby, J.-G., Le Bras, A., Douté, S., & Schmitt, B. 2001, A&A, 376, 310
Sagan, C., & Khare, B. N. 1979, Nature, 277, 102
Sheppard, S. S., & Jewitt, D. C. 2002, AJ, 124, 1757
Strazzulla, G. 1998, in Solar System Ices, ed. B. Schmitt, C. de Bergh, & M. Festou (Dordrecht: Kluwer), 281
Torbett, M. V. 1989, AJ, 98, 1477